

# Testing mechanistic explanations of observed correlations between environmental factors and marine fisheries

A.E. Gargett, M. Li, and R. Brown

**Abstract:** Based on observed correlations, marine fisheries are often hypothesized to depend on environmental factors. Since correlations are unreliable as a predictive tool, it is desirable to seek mechanistic explanations for observed correlations. This paper considers methods available for testing such mechanistic explanations. As a specific example, we consider the optimal stability window, proposed as a mechanistic explanation of observed correlations between the survival of North Pacific salmon stocks and the state of the atmosphere over the North Pacific in winter, as applied to the coastal waters and fisheries of southern British Columbia, Canada.

**Résumé :** À cause des corrélations que l'on observe entre les facteurs de l'environnement et les pêches marines, on émet souvent l'hypothèse qu'il existe un lien de dépendance entre les deux. Cependant, comme les corrélations ne peuvent servir d'outil fiable pour établir des prédictions, il faut rechercher des explications mécanistes aux corrélations observées. Nous présentons ici un examen des méthodes disponibles pour tester de telles explications mécanistes. L'exemple précis que nous étudions est la « fenêtre de stabilité maximale » qui a été proposée comme explication mécaniste des corrélations qui existent entre la survie des stocks de saumons du Pacifique Nord et les conditions de l'atmosphère au-dessus du Pacifique Nord en hiver et nous l'appliquons aux eaux côtières et aux pêches du sud de la Colombie-Britannique, Canada.

[Traduit par la Rédaction]

## Introduction

The study of the effects of climate variation on fisheries has depended heavily on correlations between fisheries data, generally catch, and some environmental variable(s). While correlations are suggestive, they are notoriously unreliable as predictive tools (Kinsman 1957). Without knowing the mechanistic connections between the variables being correlated, we cannot have confidence that the correlations will continue, and indeed they often fail abruptly. It is thus essential to move on to a process in which two things will happen. First, we will use correlations less as predictive measures and more as clues that signal and constrain possible mechanistic connections. Second, we will seek to test hypothesized connections.

An example of the first step in such a process is the optimal stability window proposed by Gargett (1997) as a mechanistic explanation of two correlational clues: first, positive correlation (Beamish and Bouillon 1993) on decadal time scales between North Pacific all-nation salmon catch and an index of the average strength of the wintertime Aleutian Low pressure system and, second, negative correlation (Francis and Sibley 1991) between survival of northern

(Alaska) and southern (Washington, Oregon, and northern California) stocks. Gargett (1997) argued that variations in atmospheric circulation between strong and weak phases of the Aleutian Low produce in-phase changes in coastal water column stability through coupled changes in freshwater input to the subpolar coastal ocean and wind-driven boundary upwelling in the subtropical coastal ocean. Through stability-induced changes in nutrient and light supplies to primary production, reflected in secondary production, in-phase variation of coastal stability in the eastern North Pacific translates into conditions favoring survival of juveniles entering the coastal ocean in the northern (southern) part of the salmonid range during strong (weak) Aleutian Lows, thus accounting for both correlational clues (for further details, see Gargett 1997).

Using this mechanism as an example, the present paper investigates methods for the second step, testing. To focus discussion, we consider the coastal waters and salmon stocks of southern British Columbia, Canada (Fig. 1), both offshore waters along the western coast of Vancouver Island and protected waters inside the Strait of Georgia.

## Methods

### Stability time series from in-water data

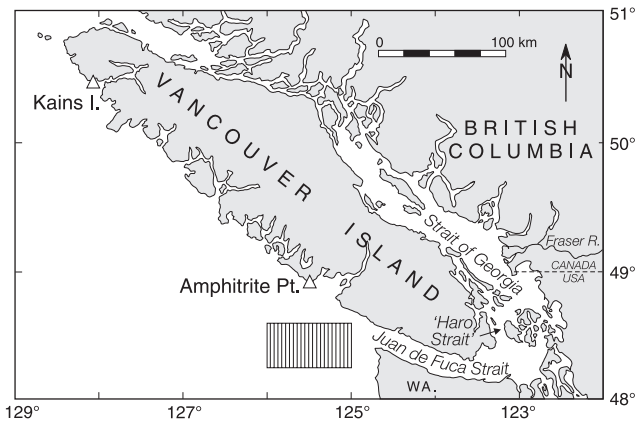
The possibility of obtaining adequate time series from CTD/bottle data inventories is explored using a test area just off the mouth of Juan de Fuca Strait (Fig. 1). This area is as well sampled as any region of the British Columbia coast because it includes the inner end of "Line P" (a line of stations sampled a minimum of three or four times per year since 1956) as well as part of a more recent grid of repeated coastal observations. Density

Received April 7, 2000. Accepted October 4, 2000. Published on the NRC Research Press web site on January 4, 2001. J15708

A.E. Gargett,<sup>1</sup> M. Li, and R. Brown. Department of Fisheries and Oceans, Institute of Ocean Sciences, Patricia Bay, P.O. Box 6000, Sidney, BC V8L 4B2, Canada.

<sup>1</sup>Corresponding author (e-mail: gargetta@dfo-mpo.gc.ca).

**Fig. 1.** Map of southern coastal British Columbia, Canada, showing the area (vertical shading) in which historical CTD/bottle data were composited, the locations (triangles) of two lighthouse shore stations, and the regions (Strait of Georgia, “Haro Strait,” and Juan de Fuca Strait) incorporated in a biophysical box model.



profiles are abstracted from data in the archives of the Institute of Ocean Sciences for a spring season defined as April–May–June, when phytoplankton growth should set the table for juvenile salmon first entering the ocean. Figure 2a shows values of upper (U) and lower (L) layer average densities (in  $\sigma_t$  units) from individual profiles: lines connect averages over the highly variable number of stations available during the spring season of a particular year. Near-surface stability (Fig. 2b) is quantified by

$$\frac{\Delta\sigma_t}{\Delta z} = \frac{(\overline{\sigma_L} - \overline{\sigma_U})}{(d_L - d_U)}$$

where  $\sigma$  and  $d$  are, respectively, layer-averaged density and depth and the overbar denotes an average over all available stations within a year.

### Stability time series from surrogate data

If deep density remains constant, a surrogate time series for coastal water column stability can be obtained from measurements of surface density at shore stations. To test this possibility, we use surface density values calculated from routine daily measurements of surface temperature and salinity at the two coastal lighthouse stations shown in Fig. 1 (data available through Institute of Ocean Sciences web site <http://www.pac.dfo-mpo.gc.ca/sci/pages/lighthousedata.htm>), again averaging over the spring season.

### Salmonid catch and survival data

Records of catch and escapement of chum salmon (*Oncorhynchus keta*) entering the ocean off the west coast of Vancouver Island from 1951 to 1981 are reported in Beacham (1984). As well, we use estimates of survival of Chilko Lake sockeye salmon (*Oncorhynchus nerka*) made by direct counts of the number of smolts leaving the lake each year and the number of adults returning (predominantly) 2 years later (M.F. Lapointe, Pacific Salmon Commission, Vancouver, B.C., personal communication).

## Results

### Hypothesis testing through retrospective time series of stability

For mechanisms operating over decadal time scales, retrospective testing requires data over similar time scales. For a water column property like stability, many coastal ocean

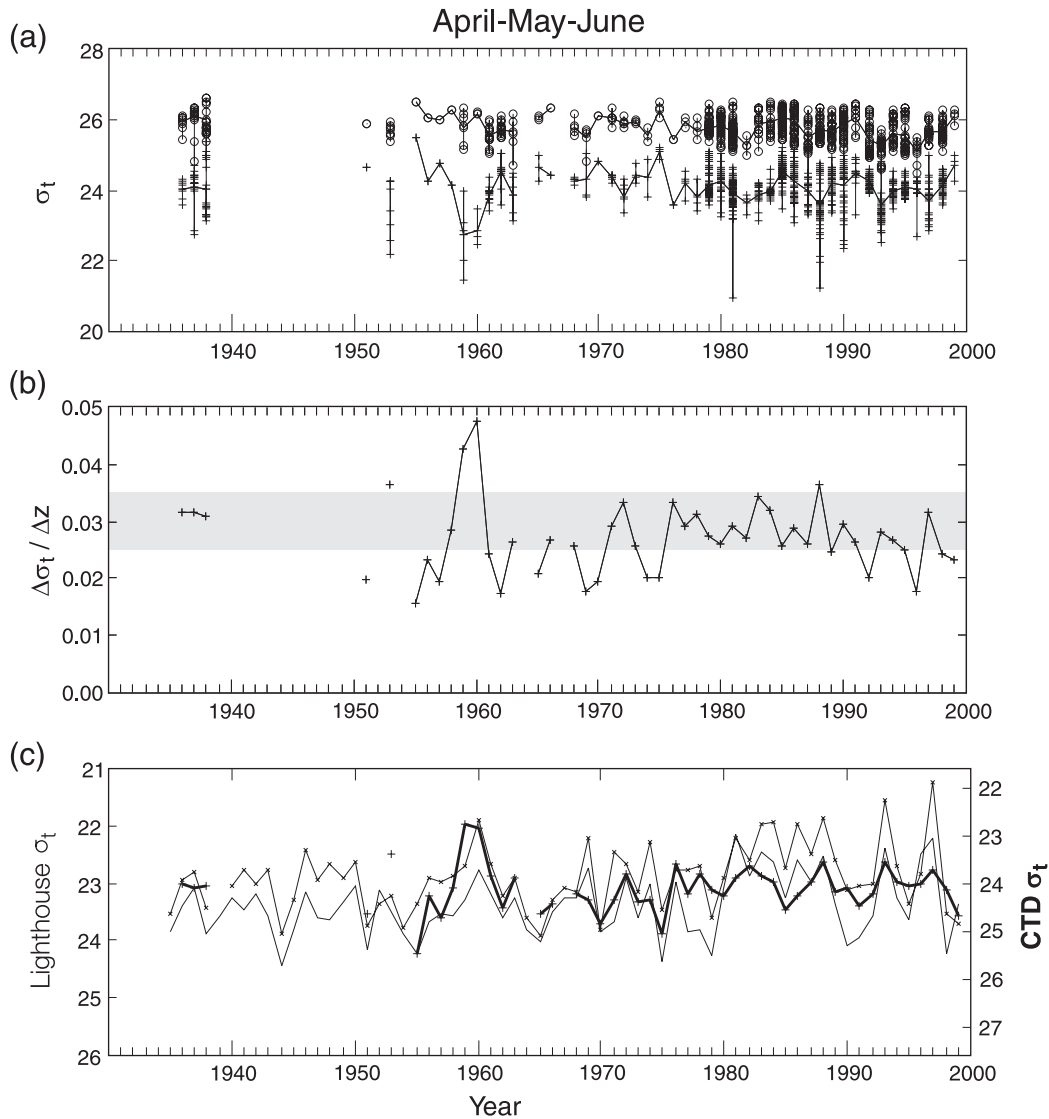
time series are well sampled only for the past 20–30 years, a period that is only about a half “cycle” of the variations in salmon catch (Beamish and Bouillon 1993). Over longer periods, the historical time series of water column density from southern British Columbia coastal waters (Fig. 2a) illustrates lack of continuity as well as undersampling, i.e., the frequent sparseness of data points in earlier years that do have data, both features typical of other coastal locations where decadal time series exist.

The time series of stability derived from this in-water data is predictably noisy, especially before sampling density increased in the early 1980s. However (disregarding for the moment the large peak in 1959–1960), there is a suggestion that stratification was generally higher during the 1980s, when northern stocks produced very large catches, and lower in the 1960s, when northern yields were poor (fig. 7 in Beamish and Bouillon 1993). Curiously, there are three relatively well-sampled years in the late 1930s: water column stability at this time, another period of high northern catches, lies at levels similar to those of the 1980s. Using these correlations as a rough calibration, Fig. 2b suggests that optimal stability in this region is  $\sim 0.03 \text{ kg}\cdot\text{m}^{-3}\cdot\text{m}^{-1}$  and that a value of  $\sim 0.02 \text{ kg}\cdot\text{m}^{-3}\cdot\text{m}^{-1}$  is suboptimal at the low-stability end of a “window.” At the beginning of the 1990s, stratification levels appear to have begun declining towards levels last seen in the 1960s (although this trend is somewhat obscured by temporary rises associated the various El Niño events of the 1990s), suggesting that during this period, coastal ocean conditions moved towards suboptimal for northern stocks.

We return now to the most obvious signal in this record, the major 1959–1960 event associated with a large decrease of surface layer density (due primarily to a decrease in salinity, augmented by a minor (20–30%) contribution from increased temperature). While impressive in magnitude, neither the spatial distribution nor the number of data points defining this feature is particularly satisfactory. The 1959 and 1960 averages include only six and three stations, respectively: of six in 1959, two were taken within 1 h of another in the same location and hence are effectively duplicates. Of the remaining independent data points, two of five and two of three, respectively, are located within the 100-m depth contour, so averages will be more heavily weighted to near-coast conditions than averages from years with more and (or) more homogeneously distributed samples. Compared with a year with a spatially even distribution of sampling sites, nearshore weighting of stations will tend to produce “unusually” low surface layer density because of the presence of a buoyant coastally trapped current driven by freshwater runoff (Thomson et al. 1989).

While the above discussion highlights problems associated with data that are sparsely and nonhomogeneously distributed in both time and space, it does not necessarily negate the occurrence of a high-stability event in near-coastal waters in 1959–1960: before rejecting this event as a sampling artifact, we have sought corroborating data. If surface layer density decreased significantly over a spatially extensive area, the change should be evident in the time series of surface density at the two lighthouse stations along the west coast of Vancouver Island, shown in Fig. 2c. Superimposed (heavy line) is surface layer density from the CTD/bottle

**Fig. 2.** (a) Density ( $\sigma_t$ ) averaged over the upper (+, 0–20 m) and lower (○, 60–80 m) layers of CTD/bottle casts taken within the shaded region of Fig. 1 during the months of April, May, and June. Lines are averages over all available data in a given year. (b) Water column stratification parameter  $\Delta\sigma_t/\Delta z$ . Shading indicates a possible range of optimal stability for this region. (c) Comparison of time series of upper layer density from the historical CTD/bottle data (heavy line, +), offset to overlap April, May, and June averages of densities determined daily at lighthouse shore stations shown in Fig. 1 (light lines: upper, Amphitrite Point; lower, Kains Island).

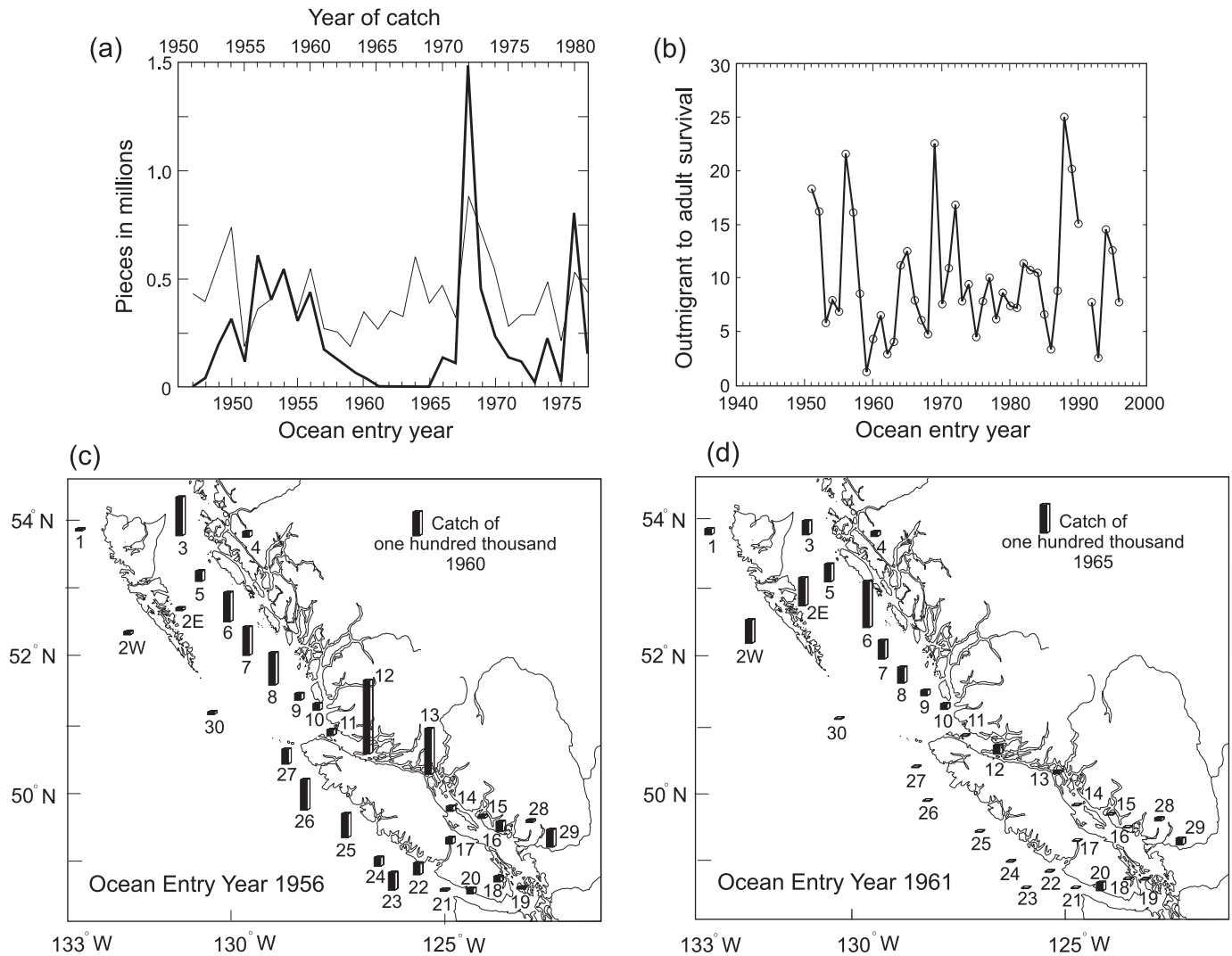


data set (an offset of 1.6  $\sigma_t$  units, chosen by eye, is necessary to produce this superposition because of the bias of the offshore CTD/bottle values to densities higher than those at the shore: all three series are plotted inversely, mimicking stability if lower layer densities remained constant). In 1960, both lighthouse stations, and particularly the southernmost station closest to the area of CTD/bottle data, show sharp maxima in inverse surface density, suggesting that the strong stability maximum seen in the offshore data during 1959 and 1960 may have extended over this larger spatial area. The additional measurements at the shore stations provide independent evidence that the 1959–1960 high-stability event in Fig. 2b is not an artifact (although the magnitude must still be considered unreliable because of the small sample size) and likely involved coastal waters along the entire length of Vancouver Island. Finally, consulting the historical record,

we realize that this stability event was likely associated with an El Niño extending from 1958 to 1960, which McGowan et al. (1998) called "...one of the largest in the past 80 years...."

Is there evidence for negative effects of this large coastal stability event on salmon stocks in southern British Columbia waters? There are few measurements of actual marine survival of salmonids; rather, most information is that of catch and escapement, the highly nonlinear results of a myriad of natural factors affecting the success of year-classes, as well as human factors interaction in their "management." Despite the uncertainties involved, catch is often used as a surrogate for marine survival; lacking other consistent records extending over decadal time scales, we continue this usage. Figure 3a is a time series of the catch of chum salmon stocks entering the coastal ocean off the west coast of Vancouver

**Fig. 3.** (a) Historical record of catch (heavy line) and escapement (light line) of chum salmon on the west coast of Vancouver Island. Ocean entry year is year of catch minus 4 years, the average time at sea. (b) Survival of sockeye salmon rearing in Chilko Lake and entering the ocean in the Strait of Georgia. Geographical distribution, by statistical area (numbered), of catch of chum salmon that entered the ocean predominantly (c) during 1956 and (d) during 1961.



Island (Beacham 1984). Since chum salmon spend 3–5 years at sea (Hartt and Dell 1986), those entering the ocean during the El Niño years of 1958–1960 returned to the catch over the period from 1961 through 1965. An abrupt decrease in allowed catch began in 1961: the fishery was progressively reduced in subsequent years and finally shut down entirely for the five years from 1965 through 1969. In the light of Fig. 2b, a possible interpretation of this period is of an ecosystem highly overstressed by the unusual combination of at least two years (1959 and 1960) on the high-stability side of optimal, immediately followed by a prolonged period (the 1960s) on the low-stability side of optimal.

Other evidence indicates that this ecosystem stress affected other salmonid species and extended over a much larger area. Figure 3b shows the survival of Chilko Lake sockeye salmon, a different species entering the coastal ocean inside southern Vancouver Island. While there are many factors at play in determining interannual survival (including conditions during extensive river migrations of this

stock to and from the ocean), note that the lowest survival in the entire record occurs for year-classes that went to sea during the 1958–1960 El Niño period, when coastal stability was high off Vancouver Island. (Since Fraser River sockeye salmon generally migrate out of the Strait of Georgia to the north, it would be preferable to relate their survival to a measurement of coastal stability further north, for example off the Queen Charlotte Islands: however, adequate data are not available in these more remote areas of the British Columbia coast.) Finally, Figs. 3c and 3d illustrate that the collapse of the chum salmon fishery documented in Fig. 3a was not confined to the west coast of Vancouver Island but extended throughout the coastal waters of southern British Columbia.

**Hypothesis testing through surrogate time series of stability**

Ocean temperature (and sometimes salinity) have been measured for several decades at various shore stations along

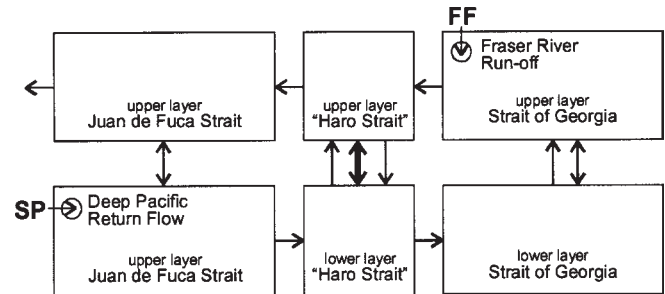
the eastern boundary of the North Pacific. If these surface observations could be used as surrogate measures of stability, they would enormously enlarge the physical database available for testing the optimal window mechanism. Unfortunately, comparison of shore station surface density records with stability data from the offshore stations used in the previous section strongly suggests that shore density *cannot* be used to make reliable surrogate estimates of stability. For example, shore station inverse surface density (Fig. 2c) reached an all-time high during the El Niño of 1997: making the necessary assumption of fixed lower layer density, this would imply that coastal ocean stability was also at an historical high. However, layer densities calculated from the offshore stations (Fig. 2a) show that to a considerable extent, surface layer density changes are echoed at depth, so that changes in vertical density *difference*, i.e., in vertical stability, are more subtle than changes in surface layer density alone. In particular, although the “true” stability of Fig. 2b does have a local maximum in 1997, the value is of the same magnitude as that typical of the early 1980s rather than an historical extreme.

#### Hypothesis testing through biophysical models

Even if the sampling density achieved in the final 15 years of Fig. 2a were to be maintained over the decades that characterize major variation in the North Pacific ocean–atmosphere system, the British Columbia coast is not an ideal place in which to look for clear evidence of the optimal window effect. This is because British Columbia coastal waters are a complicated mixture of “pure” northern and southern regimes. Studies of anomalous precipitation associated with extreme states of the Aleutian Low (Cayan and Peterson 1989) indicate that precipitation in the Pacific Northwest, including southern British Columbia, is out of phase with precipitation in the pure northern regime (Alaska). In addition, the southern British Columbia outer coast is affected by seasonal (summer) upwelling rather than the year-round upwelling characteristic of a pure southern regime (southern Oregon). The results of the previous section are at least consistent with the hypothesis that the coastal ocean off the west coast of Vancouver Island functions as a northern regime (i.e., low survival rates associated with low stability). However, the transitional nature of this area means that the clearest signature of relationships between coastal stability and salmon survival would come from Alaskan and southern Oregon – northern Californian coastal waters. As in our study area, reliable water column data from these areas are not available over the required several decades: for example, the GAK1 Alaskan shelf CTD station has only been sampled intensively since 1990, while the long CALCOFI data set does not regularly sample northern Californian waters. Moreover, at least in our study region, we have demonstrated failure of the necessary assumption of constant deepwater density that underlies potential use of longer continuous time series of surface surrogates for stability. Thus, a conclusive observational test of the optimal window hypothesis awaits many years of well-sampled repeat CTD stations in appropriate areas.

In contrast, biophysical models enable immediate exploration of mechanistic explanations of observed correlations between environmental variables and marine fish stocks. As an

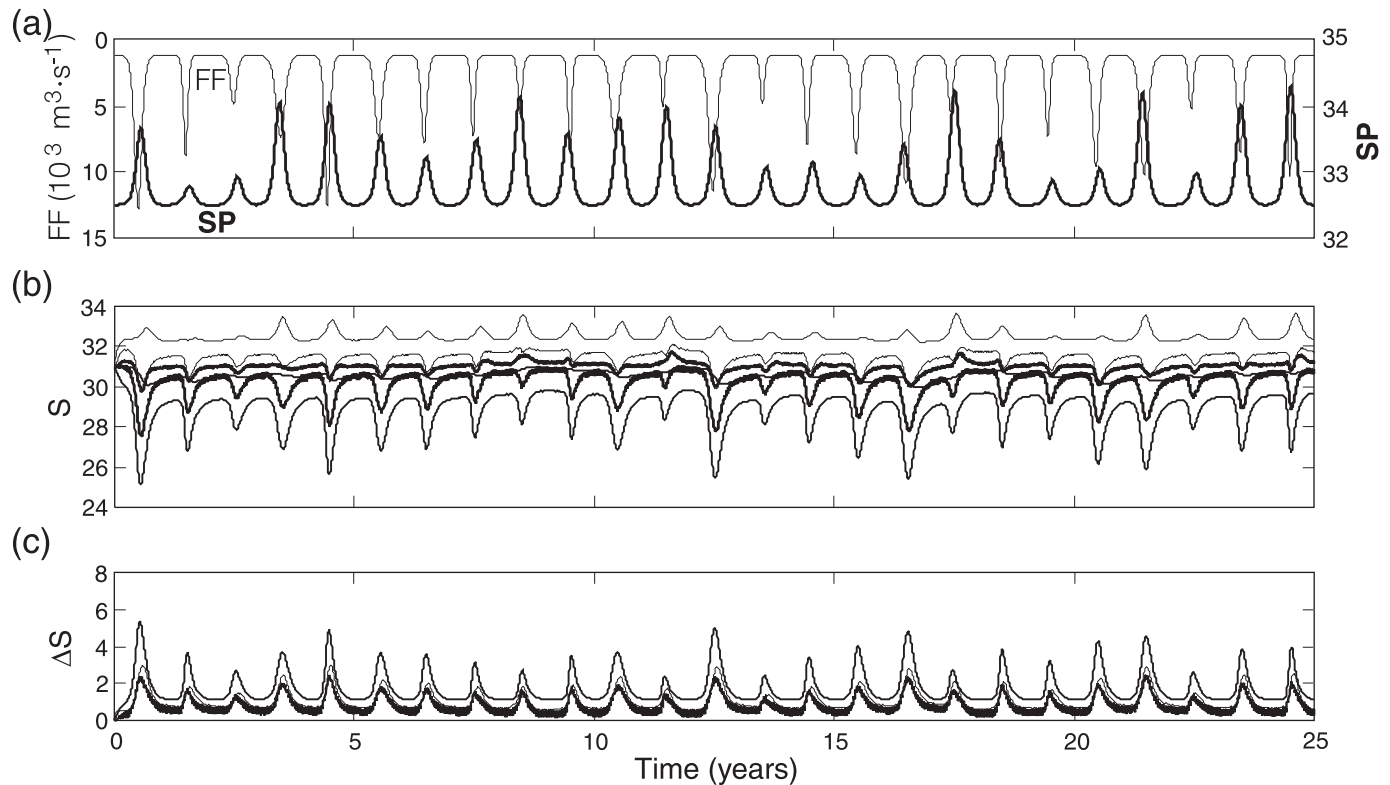
**Fig. 4.** Schematic of a box model developed to test application of the optimal stability window to the Strait of Georgia region. Upper and lower boxes represent 0–50 and 50–200 m, respectively. The model includes estuarine circulation (unidirectional arrows) forced by freshwater input (FF) to the upper Strait of Georgia box and vertical mixing (bidirectional arrows). Salinity of the deep return flow in the lower Juan de Fuca Strait box is restored to Pacific salinity (SP).



example of such use of models, we focus a process modelling study on the Strait of Georgia (Fig. 1), the body of water between Vancouver Island and the mainland coasts of British Columbia and Washington State, and the region of first ocean contact for major Fraser River salmon stocks. We first determine what the window hypothesis predicts for this region. Cayan and Peterson (1989) demonstrated that when Alaska is wet (strong Aleutian Low), the Pacific Northwest is dry. Thus, assuming that the Strait of Georgia is a northern (light-limited) region, the optimal window predicts that Fraser stocks should vary out of phase with northern British Columbia and Alaska stocks. However, the Strait of Georgia actually functions as a *southern* regime because high stability associated with freshet of the Fraser River regularly leads to nutrient limitation of primary production in the late spring – early summer season when juvenile salmon first enter the coastal ocean. In a southern regime, low freshwater input associated with a strong Aleutian Low results in low stability and moves primary production towards more favorable conditions (see Gargett 1997). The window hypothesis thus predicts that Fraser River stocks entering the Strait of Georgia during favorable conditions associated with a strong Aleutian Low and migrating northwards where conditions continue favorable should be strong when northern stocks are strong. While this prediction agrees with observations for the dominant Fraser River sockeye stocks (Beamish et al. 1997), we will use a simple biophysical model to examine whether the Strait of Georgia system actually works this way.

Figure 4 shows the physical configuration of a simple box model of the Strait of Georgia (G) and the relatively narrow passages that are its major connection to the offshore Pacific: first the many tidal mixing channels (H) labelled “Haro Strait” in Fig. 1 and then the broad Juan de Fuca Strait (F). We believe that such a minimalist model is (i) an appropriate first step in the study of decadal time scales (more complex models being too expensive to run for long periods of time), (ii) an essential tool for exploration of sensitivities to poorly known biological parameters, and (iii) the maximum degree of model complexity likely to be constrained by sparse available data.

**Fig. 5.** Twenty-five-year simulation of salinity and stability fields produced by stochastic forcing of the physical model. (a) Stochastic physical forcing fields of Fraser River flow (FF, light line) and deep Pacific salinity (SP, heavy line). (b) Resulting time series of salinity  $S$  for the six model boxes. Line width identifies the basin (heavy lines, “Haro Strait”; medium lines, Strait of Georgia; light lines, Juan de Fuca Strait). In each basin pair, the upper layer has the lower  $S$ . (c) Stability, represented by the difference  $\Delta S$  between upper and lower box salinities. Line width convention is the same as in Fig. 5b.



This estuarine box model, described in detail by Li et al. (1999) and subsequently referred to as the GHF model, is forced by strongly seasonal freshwater flow into the upper (0–50 m) G box, with salinity balance maintained by restoring salinity of the deep (50–200 m) F box to a “Pacific” salinity, which also varies seasonally as upwelling moves more saline water onto the British Columbia shelf in summer (Freeland and Denman 1982). Within the H boxes, strong tidal mixing with imposed variation due to the spring–neap tidal cycle (Griffin and LeBlond 1990) is modulated by model stability.

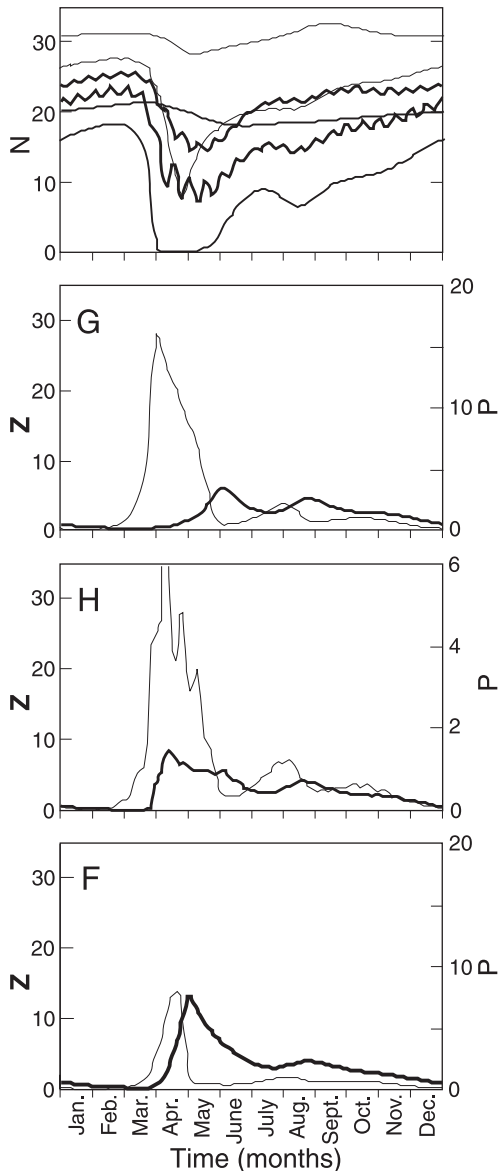
The single coefficient parameterizing the density-driven exchange flow is chosen to produce a response time to changes in freshwater flow of order 1 year (England et al. 1996). Forced with average annual cycles of freshwater flow and Pacific salinity based on observations, the model reproduces the observed seasonal cycle of average salinities in the six boxes. To investigate variability, the average solution is then perturbed by allowing significant parameters describing the physical forcing to vary within bounds, which are reasonably well determined from observations (Appendix A). As shown in Fig. 5, variability in physical forcing results in considerable interannual variability in the salinity fields, especially that of the upper Strait of Georgia, where stability varies by as much as a factor of 2.

When a simple nitrate–phytoplankton–zooplankton biological module (Li et al. 2000) is coupled to the steadily forced physical model, reasonable choices of biological pa-

rameters lead to an acceptable picture of the average annual biological cycles in the system (Fig. 6), as far as these are constrained by observations. In the Strait of Georgia, a spring bloom initiated by increasing light level is followed by a minimum in phytoplankton biomass caused partly by nutrient limitation and partly by zooplankton grazing; a secondary late summer peak of phytoplankton occurs as nitrate levels are renewed by input from offshore upwelling (see Appendix A for model implementation). Levels of phytoplankton are much lower (note the scale difference) in Haro Strait, where strong vertical mixing on spring tides causes regular losses to the unlit lower layer. With a very abbreviated spring bloom of much smaller magnitude than that in the Strait of Georgia, the ecosystem in Juan de Fuca Strait approaches high-nutrient, low-chlorophyll characteristics of the offshore Northeast Pacific (Miller 1993).

Figure 7 illustrates the response of this simple biological system to the interannual variation in physical properties shown in Fig. 5. Observationally reasonable interannual variability in the physical environment does not produce comparable variability in phytoplankton or zooplankton standing stocks in the Strait of Georgia, i.e., weaker (stronger) stratification does *not* produce significantly larger (smaller) zooplankton biomass as food for juvenile salmon. The model shows that the optimal window hypothesis is *not* valid for this system because local stratification-modulated mixing processes, on which the optimal window hypothesis is based, are not the dominant physical processes supplying nutrients to the

**Fig. 6.** Characteristic annual cycles of biological variables from a nitrate (N) – phytoplankton (P) – zooplankton (Z) model coupled to the physical box model of Fig. 4. Top panel: nitrate cycles in all six boxes. Line width convention is the same as in Fig. 5. All biological variables are in nitrate units of  $\text{mmol NO}_3\text{-m}^{-3}$ . Lower panels: upper layer values of modelled phytoplankton (light line) and zooplankton (heavy line) biomass in the Strait of Georgia (G), “Haro Strait” (H), and Juan de Fuca Strait (F).



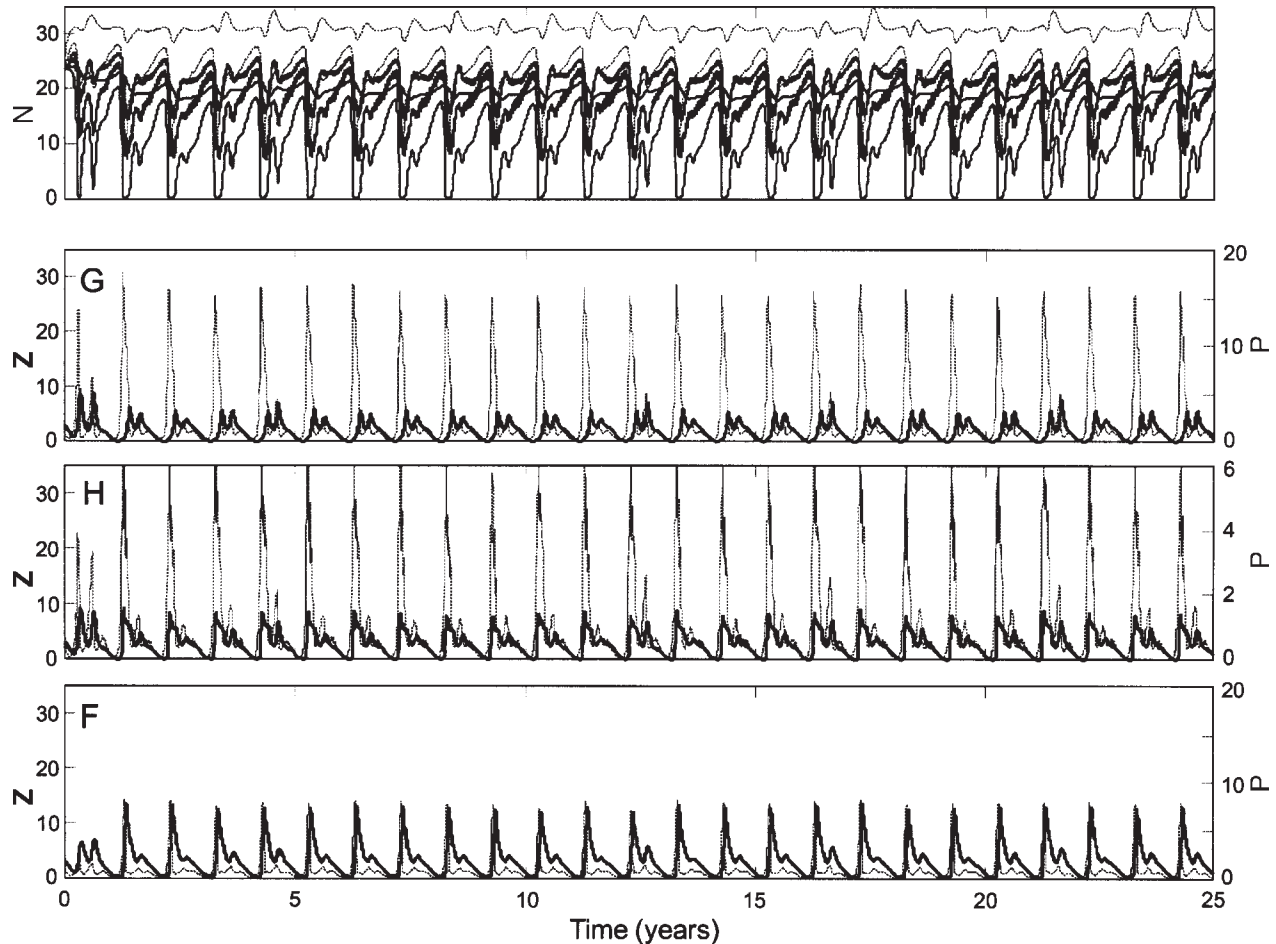
euphotic zone in the Strait of Georgia. Instead, density-driven advection dominates vertical diffusion in supplying nutrients to this strongly estuarine system. Increased freshwater forcing of the upper Strait of Georgia produces an increased seaward pressure gradient, which drives stronger estuarine exchange flow. While the increased upwelling of nutrient-rich deep water within the Strait of Georgia thus supplies new nutrient to the surface layer in the Strait of Georgia at a rate that is higher than normal, the increased phytoplankton biomass suffers a higher than average

advective loss in the outward-flowing surface layer. The opposite balancing of processes occurs when freshwater forcing is decreased. The net result is insensitivity of modelled phytoplankton and zooplankton biomass within the Strait of Georgia to variations in freshwater forcing of magnitudes comparable with those that might be expected due to decadal variability in the wintertime Aleutian Low pressure system.

Nevertheless, Fraser River salmon stocks *do* vary dramatically, and the variations *are* apparently correlated with atmosphere–ocean variability on decadal time scales, with the same phase as northern stocks. If the optimal window hypothesis is not the explanation, what is? Simple models allow us not only to disprove hypotheses, but also to explore other possibilities. The simplicity and speed of the box model allowed extensive sensitivity studies (Li et al. 2000) which revealed that large ecosystem changes *can* be induced by relatively small changes in the biological rate parameters, specifically phytoplankton growth rate, zooplankton growth rate, and zooplankton mortality rate. The latter is arguably the most poorly known of the three, including as it does effects of predation losses as well as natural mortality. Figure 8 illustrates the effects of allowing stochastic variation of zooplankton mortality rate (see Appendix B) in a multi-year simulation with fixed physical forcing, hence a constant annual cycle of all physical variables. The biological fields now exhibit greatly increased interannual variability, particularly pronounced in the Strait of Georgia, where there are many “normal” years with spring peaks of phytoplankton and zooplankton but also a year (asterisk) of large phytoplankton standing stocks (and almost no zooplankton) throughout the lighted seasons of the year, followed immediately by a year in which the spring bloom of phytoplankton is greatly reduced in both magnitude and extent but zooplankton biomass is not obviously different from normal.

When trying to decide whether Fig. 8 exhibits perhaps too much interannual variability, we begin to appreciate the dearth of observational data with which to validate biological model results, whether they come from simple and cheap box models like the present one or from much more complex and expensive models with high spatial resolution and more “realistic” biology. In the entire GHF system, there are very few measurements of annual cycles of nitrate, fewer such measurements of phytoplankton and (or) zooplankton biomass, and even fewer measurements of the interannual variability of these quantities. For the GHF system, there are only fragments of the kind of data needed for model validation. However, the existing fragments suggest that the interannual biological variability produced by this simple model is reasonable in both character and magnitude. Figure 9 shows two consecutive years of monthly phytoplankton and zooplankton measurements taken by Stockner et al. (1979) at a grid of stations in the southern Strait of Georgia. In spring 1975, both phytoplankton and zooplankton standing stocks are strongly peaked, a “normal” seasonal cycle for the Strait of Georgia (Fig. 6). However, in the very next year, phytoplankton stocks are significantly larger and remain at these levels throughout the lighted season, while zooplankton standing stock is low. Similar behaviors have already been pointed out in the simulation results shown in Fig. 8.

**Fig. 7.** Biological time series resulting from the 25-year model run with stochastic physical forcing shown in Fig. 5 and constant biological parameters. Line width conventions are the same as in Fig. 5; abbreviations are the same as in Fig. 6. All variables are in nitrate units of  $\text{mmol NO}_3\text{-m}^{-3}$ .



Investigation of the GHF biological–physical system, as represented by our box model, leads us to conclude that in a strongly estuarine system, reasonable variability in physical forcing will not translate directly into large changes in zooplankton standing stocks and hence cannot be a *direct* cause of large variation in juvenile salmon survival based on food availability. However, small changes in poorly known biological rate parameters can produce large interannual variations in zooplankton standing stock, variations consistent in both pattern and levels with available observational data in the Strait of Georgia. Thus, if the physical environment *does* produce a significant effect on the output of the biological system in the Strait of Georgia, it apparently does so only indirectly, through effect(s) of physical processes on biological rate parameters.

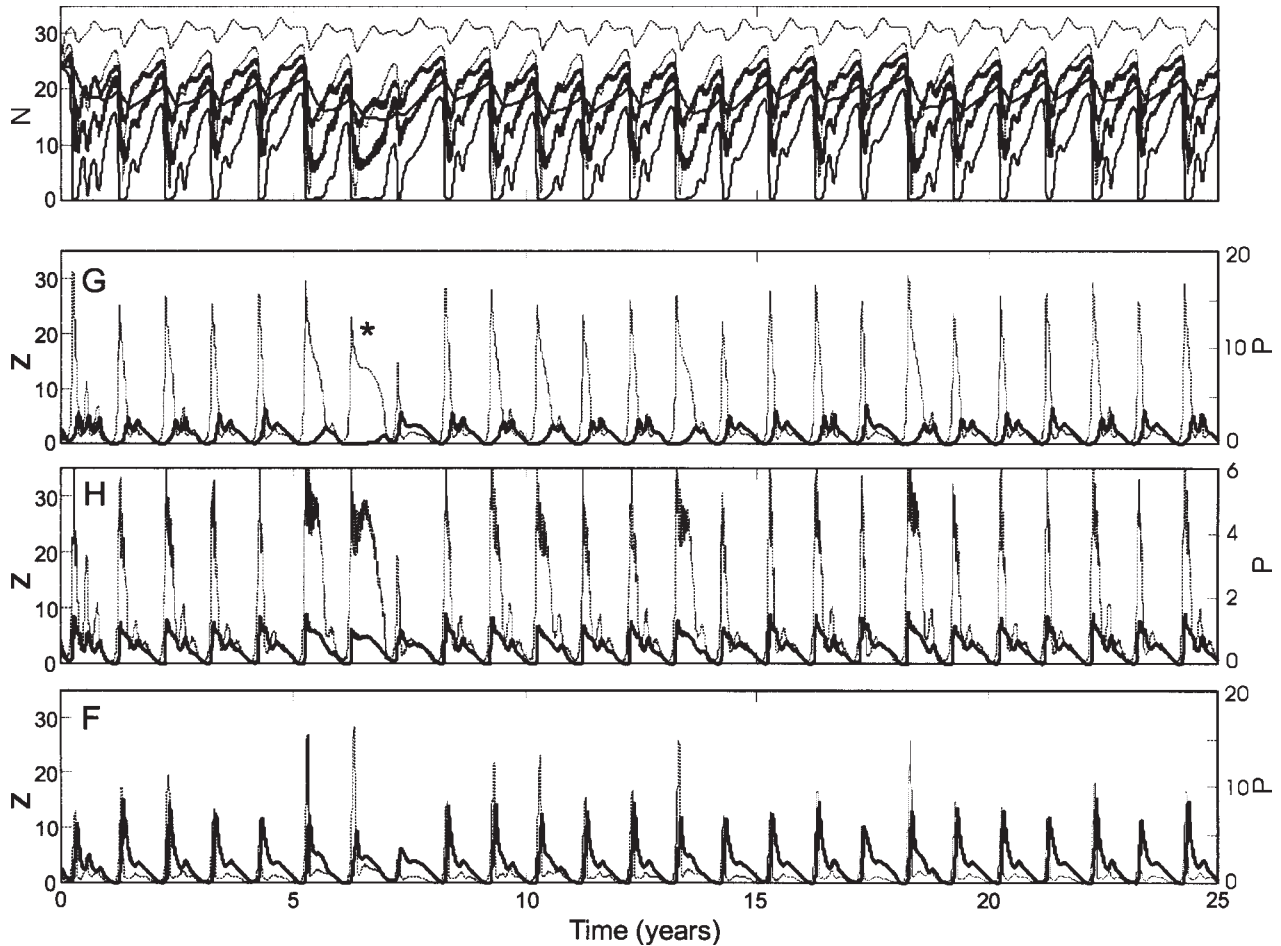
One obvious way in which estuarine physical processes can affect biological rate parameters is through the silt content of freshwater forcing, itself linked to atmospheric forcing on both interannual and decadal time scales. As illustrated in Fig. 10 for the Fraser River, suspended sediment transport typically varies strongly with river flow, whether measured by annual peak or annual mean values. Thus, in years of stronger than average freshwater input to catchment areas, river plumes entering estuarine regions not only cover larger areas, but also carry higher suspended

loads. Such suspended material will arguably influence all three of the fundamental growth rates involved in zooplankton production. Suspended sediment will affect the light environment in which phytoplankton grow, thus affecting the phytoplankton growth rate. Because zooplankton mechanically sense and capture their prey, an increased percentage of nonfood (sediment) particles in their environment should decrease zooplankton growth rate. However, poorer zooplankton growth may be partially or completely offset by decreased predation losses (zooplankton mortality rate), as higher sediment concentration degrades the visual environment in which larval fish search for and capture their prey. Which of these diverse impacts will dominate change in productivity of a highly nonlinear marine ecosystem is an important question for future investigation.

## Discussion

This paper has considered various methods for testing the optimal stability window (Gargett 1997) as a mechanistic underpinning for observed correlations between North Pacific salmon catch and variation in atmospheric forcing of the ocean. We first considered the use of retrospective analyses of historical in-water data to establish a connection between water column stability and marine survival of salmon.

**Fig. 8.** Biological time series resulting from a 25-year model run with constant annual cycle of physical forcing (identical annual cycles of physical variables) and stochastic variation of zooplankton mortality rate. Line width conventions are the same as in Fig. 5; abbreviations are the same as in Fig. 6. All variables are in nitrate units of  $\text{mmol NO}_3\text{-m}^{-3}$ .

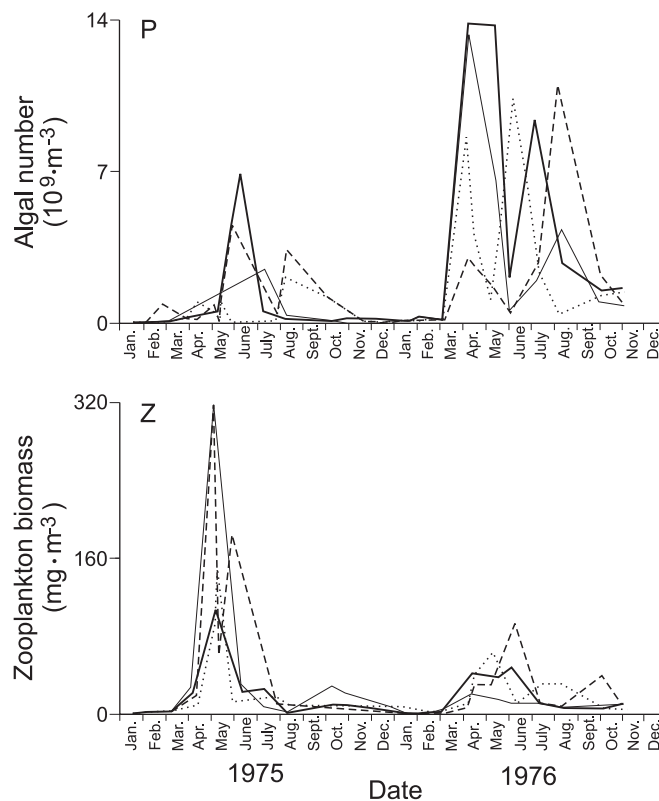


Results from a coastal area off the west coast of Vancouver Island suggest that this outer coastal region acts as a northern regime, with an optimal window in stability centered around  $\sim 0.03 \text{ k}\cdot\text{m}^{-3}\cdot\text{m}^{-1}$ . When stability is near this value, during the late 1930s and the 1980s, northern stocks on average produced large catches. Northern catches were low during periods when stability fell below this level, e.g., during the 1960s, or substantially exceeded it, e.g., 1959–1960. While this analysis is suggestive, problems of data density in both time and space made it difficult to form reliable time series of water column stability over the required decadal time scales, even in the “well-sampled” region examined. Continuously sampled time series of temperature and (or) salinity at various shore stations are a potential source of longer surrogate records of stability for use in testing the window hypothesis but prove unsatisfactory for two reasons. First, the necessary assumption of constant lower layer properties is unfounded, at least in the British Columbia coastal area that we have examined. Second, it could become necessary to use a surrogate for a surrogate in northern regions, where density is dominated by salinity but long time series of surface salinity are rarely available. (Dis)proof of the stability window mechanism from observed water column properties awaits establishment and maintenance of re-

peat CTD stations in the coastal ocean at the northern and southern limits of the range of North Pacific salmonids and another full “cycle” of decadal variation in atmospheric forcing.

In the meantime, even very simple models of the biological–physical system in smaller domains may provide important tests of the optimal window hypothesis; in the region that we modelled, it failed. Nonetheless, the focused process of attempting to test the hypothesis provided a framework for understanding why it failed (because the strongly estuarine physics of the modelled system differed significantly from the physics underlying the original window hypothesis). The model developed in the process of testing also provided a tool for exploring other mechanisms by which the physical ocean environment, itself forced by the atmosphere, could affect marine productivity. We suggest that in strongly estuarine environments such as the Strait of Georgia, variability in atmospheric delivery of freshwater to the estuarine catchment area could cause associated variability in marine primary and secondary productivity through effects of silt content on biological rate parameters. Because the zooplankton production that supports marine fisheries depends on both phytoplankton and zooplankton rate parameters, the phase of any relationship between freshwater input and pro-

**Fig. 9.** Strong interannual variability, similar to that observed in model runs with stochastic zooplankton mortality rates (cf. Fig. 8), is seen in two consecutive years of phytoplankton (P) and zooplankton (Z) observations taken monthly over a grid of stations in the southern Strait of Georgia (Stockner et al. 1979). Stations: 5, heavy solid line; 6, light solid line; 7, dotted line; 8, broken line.



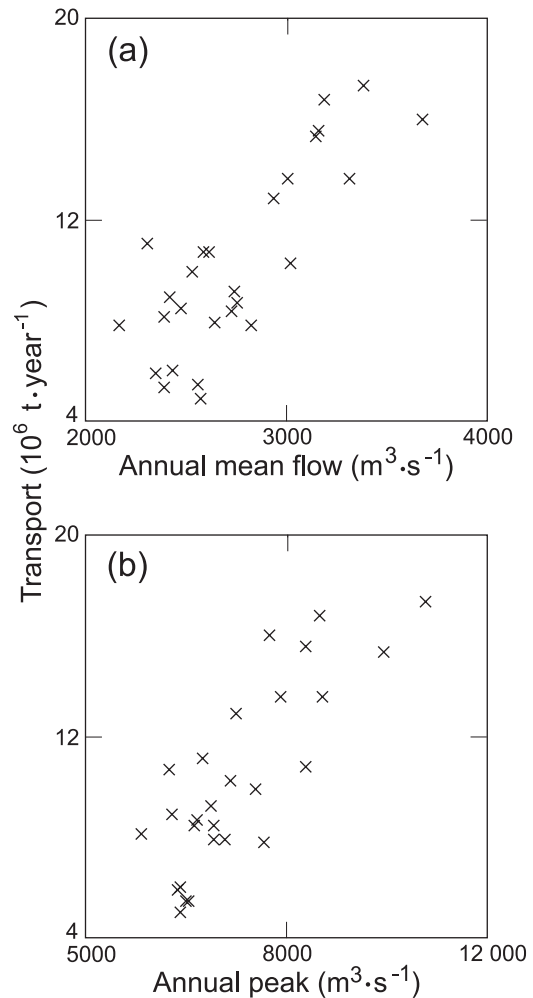
ductivity will depend on the net result of these indirect effects of the physical environment on all relevant rate parameters.

The results of this attempt to test the optimal window hypothesis are mixed. On the outer coast of southern Vancouver Island, available historical data appear at least consistent with an assumption that this region acts as a northern regime with maximum production of salmon occurring within an optimal range of water column stability. In contrast, a model of the Strait of Georgia shows that the biological productivity of this region is not determined by the physical processes assumed to underlie the optimal window hypothesis. On the basis of these results, we suggest that the optimal window hypothesis will be applicable as a predictive tool in areas where juvenile salmon enter the coastal ocean directly but inapplicable in other regions where they spend the first few to several weeks of their ocean lives in a strongly estuarine environment.

### Acknowledgments

We thank Ron Perkin for maintaining the British lighthouse data, Skip McKinnell for accessing the Chilko Lake time series, and Ken Denman for his contribution to the GHF box model.

**Fig. 10.** Variation of the suspended sediment (clay plus silt) load carried into the Strait of Georgia by the Fraser River as a function of (a) mean annual flow and (b) annual peak flow (sediment data, 1966–1992, courtesy of M. Church, Geography Department, University of British Columbia, Vancouver, B.C.).



### References

- Beacham, T.D. 1984. Catch, escapement, and exploitation of chum salmon in British Columbia, 1951–1981. Can. Tech. Rep. Fish. Aquat. Sci. No. 1270. (Department of Fisheries and Oceans, Fisheries Research Branch, Pacific Biological Station, Nanaimo, BC V9R 5K7, Canada.)
- Beamish, R.J., and Bouillon, D.R. 1993. Pacific salmon production trends in relation to climate. Can. J. Fish. Aquat. Sci. **50**: 1002–1016.
- Beamish, R.J., Neville, C.-E.M., and Cass, A.J. 1997. Production of Fraser River sockeye salmon (*Oncorhynchus nerka*) in relation to decadal-scale changes in the climate and the ocean. Can. J. Fish. Aquat. Sci. **54**: 543–554.
- Cayan, D.R., and Peterson, D.H. 1989. The influence of North Pacific atmospheric circulation on streamflow in the west. Geophys. Monogr. **55**: 375–397.
- England, L.A., Thomson, R.E., and Foreman, M.G.G. 1996. Estimates of seasonal flushing times for the southern Georgia Basin. Can. Tech. Rep. Hydrogr. Ocean Sci. No. 173. (Department of

- Fisheries and Oceans, Institute of Ocean Sciences, P.O. Box 6000, Sidney, BC V8L 4B2, Canada.)
- Francis, R.C., and Sibley, T.H. 1991. Climate change and fisheries: what are the real issues? *Northwest Environ. J.* **7**: 295–307.
- Freeland, H.J., and Denman, K.L. 1982. A topographically controlled upwelling centre off Vancouver Island. *J. Mar. Res.* **40**: 1069–1093.
- Gargett, A.E. 1997. The optimal stability “window”: a mechanism underlying decadal fluctuations in North Pacific salmon stocks? *Fish. Oceanogr.* **6**: 109–117.
- Griffin, D.A., and LeBlond, P.H. 1990. Estuary/ocean exchange controlled by spring–neap tidal mixing. *Estuarine Coastal Shelf Sci.* **30**: 275–297.
- Hartt, A.C., and Dell, M.B. 1986. Early oceanic migrations and growth of juvenile salmon and steelhead trout. *Int. North Pac. Fish. Comm. Bull. No. 46.* (International North Pacific Fisheries Commission, 6640 Northwest Marine Dr., Vancouver, BC V6T 1X2, Canada.)
- Kinsman, B. 1957. Proper and improper use of statistics in geophysics. *Tellus*, **9**: 408–418.
- Li, M., Gargett, A.E., and Denman, K.L. 1999. Seasonal and interannual variability of estuarine circulation in a box model of the Strait of Georgia and Juan de Fuca Strait. *Atmos.–Ocean*, **37**: 1–19.
- Li, M., Gargett, A.E., and Denman, K.L. 2000. What determines seasonal and interannual variability of phytoplankton and zooplankton in strongly estuarine systems? Application to the semi-enclosed estuary of Strait of Georgia and Juan de Fuca Strait. *Estuarine Coastal Shelf Sci.* **50**: 467–488.
- McGowan, J.A., Cayan, D.R., and Dorman, L.M. 1998. Climate–ocean variability and ecosystem response in the North-East Pacific. *Science (Washington, D.C.)*, **281**: 210–217.
- Miller, C.B. 1993. Pelagic production processes in the Subarctic Pacific. *Prog. Oceanogr.* **32**: 1–15.
- Stockner, J.G., Cliff, D.D., and Shortreed, K.R.S. 1979. Phytoplankton ecology of the Strait of Georgia, British Columbia. *J. Fish. Res. Board Can.* **36**: 657–666.
- Thomson, R.E., Hickey, B.M., and LeBlond, P.H. 1989. The Vancouver Island Coastal Current: fisheries barrier and conduit. *Can. Spec. Publ. Fish. Aquat. Sci. No. 108.* pp. 256–296.

## Appendix A. Stochastic variability of physical forcing of the GHF box model

Fraser River freshwater input to the Strait of Georgia model is represented by the functional form freshwater flow (FF) (cubic metres per second)

$$FF(t) = F_w + F_f \operatorname{sech}^2\left(\frac{t - t_p}{t_w}\right)$$

where winter flow  $F_w = 10^3 \text{ m}^3 \cdot \text{s}^{-1}$  is constant and  $F_f$  is the peak of freshet flow above  $F_w$ ,  $t_p$  is the time of peak freshet flow, and  $t_w$  is its time extent; all are considered stochastic variables of the generic description

$$v = v_o + v_r \text{ svar}$$

where svar is a random variable uniformly distributed in [0,1]. Table A1 shows values of  $v_o$  and  $v_r$  for the three variables, chosen from historical records of Fraser River flow. The functional form  $FF(t)$  is multiplied by a factor of 1.5 (Griffin and LeBlond 1990) to allow for covarying flow of other rivers and streams into the Strait of Georgia.

**Table A1.** Offset ( $v_o$ ) and range ( $v_r$ ) values for the stochastic model parameters describing interannual variability in physical forcing.

	$v_o$	$v_r$
$F_f$ ( $\text{m}^3 \cdot \text{s}^{-1}$ )	$3 \times 10^3$	$8 \times 10^3$
$t_p$ (months)	5	1
$t_w$ (months)	3	1
$S_u$	0	2
$t_{\text{lag}}$ (months)	0	2

The second forcing function, that of the “deep Pacific salinity” towards which the salinity of the deep F box is continuously restored, represents an annual cycle imposed by summer upwelling of high-salinity California Undercurrent water:

$$SP(t) = S_w + S_u \operatorname{sech}^2\left(\frac{t - t_p - t_{\text{lag}}}{t_u}\right)$$

where base (winter) salinity  $S_w = 32.5$  and time extent  $t_u = 3$  months of the upwelling period are fixed but  $S_u$ , the maximum salinity increase associated with upwelling, and  $t_{\text{lag}}$ , the time lag between the time  $t_p$  of Fraser freshet peak (itself a stochastic variable, see above), are stochastic variables. Values in Table A1, resulting in maximum (summer) values between 32.5 and 34.5, were based on a compilation of historical salinity data for the “deep” (depth >50 m) Juan de Fuca Strait (W.R. Crawford, Institute of Ocean Sciences, Sidney, B.C., personal communication). Because water upwelled in summer is high in nutrients as well as salinity, the model also restores the nitrate of the deep Juan de Fuca box to a seasonally varying function derived from the above salinity function and the deep nitrate–salinity correlation shown by Mackas and Harrison (1997, their fig. 6a).

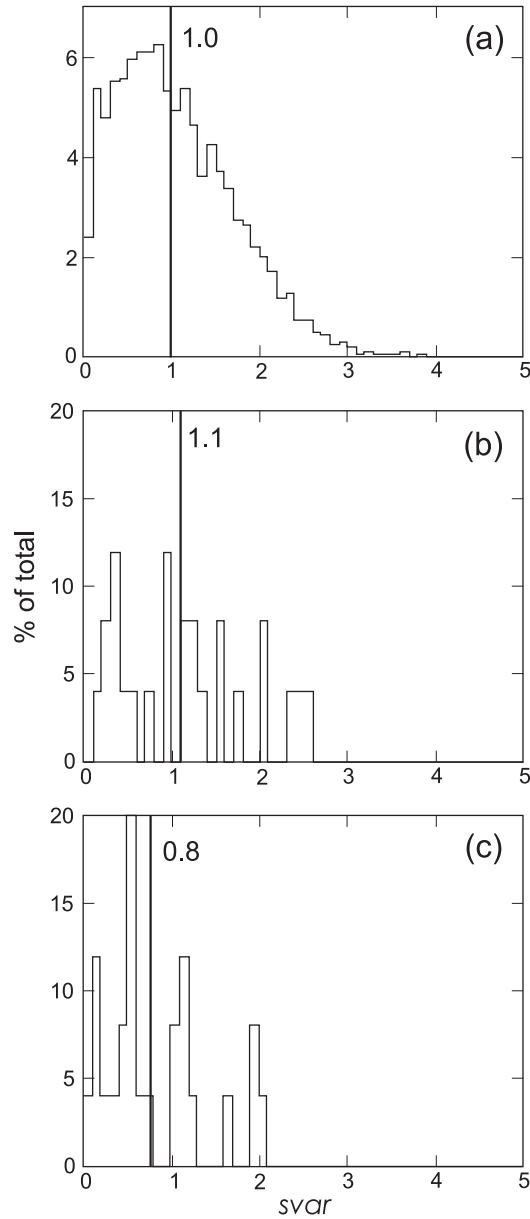
## Appendix references

- Griffin, D.A., and LeBlond, P.H. 1990. Estuary/ocean exchange controlled by spring–neap tidal mixing. *Estuarine Coastal Shelf Sci.* **30**: 275–297.
- Mackas, D.L., and Harrison, P.J. 1997. Nitrogenous nutrient sources and sinks in the Juan de Fuca Strait/Strait of Georgia/Puget Sound estuarine system: assessing the potential for eutrophication. *Estuarine Coastal Shelf Sci.* **44**: 1–21.

## Appendix B. Distribution function for stochastic zooplankton mortality rate

In model runs with stochastic variation of zooplankton mortality rate ( $z_m$ ), individual values are specified by  $z_m = (\text{svar})z_{\text{mo}}$ , where  $z_{\text{mo}}$  is a constant and svar is a stochastic variable. Since biological rates are positive definite, appropriate stochastic values must be chosen from a single-sided distribution function. To generate such a distribution function, we use a normal distribution with mean  $m_n = 1$  and standard deviation  $\sigma_n = 1.5$ . Individual values  $z_m$  chosen from this parent population (as returned by the MATLAB random number generator *randn*) are *discarded* unless the mortality rate is both positive and larger than the realized growth rate (while the mortality rate may temporarily exceed achieved growth, it cannot do so on average). Accepted val-

**Fig. B1.** (a) “Discarded normal” distribution suitable for generating (positive definite) biological rates. The large-sample (5000-point) mean has been normalized to 1.0. (b) and (c) Consecutive 25-point samples chosen from the discarded normal distribution illustrate the well-known fact that small-sample (25-point) means may differ substantially from both the large-sample mean and each other.



ues form the “discarded normal” distribution seen in Fig. B1a normalized to a large-sample mean of 1.0. While other positive definite distributions may be generated, the discarded normal distribution seems a reasonable (perhaps conservative) first-order description of variability in the underlying mortality rate.

It should be noted that means over small samples (such as the 25 values used in the “long” 25-year runs considered in this paper) may differ considerably from the large-sample mean of  $1.0z_{mo}$ . Consecutive selection of two 25-value sets (Figs. B1b and B1c) yielded means of roughly  $1.1z_{mo}$  and  $0.8z_{mo}$ , the latter equal to the small-sample mean for the run shown in Fig. 9. Much larger deviations are possible.